Collapse-driven large eruptions

Agust Gudmundsson

Department of Earth Sciences, Royal Holloway University of London, Egham TW20 0EX, UK (a.gudmundsson@es.rhul.ac.uk)

Published in Journal of Volcanology and Geothermal Research, August 2015

Abstract

For a typical poroelastic shallow crustal magma chamber, about 0.1%, of the mafic magma and about 4% of the felsic magma is erupted and/or injected during magma-chamber rupture. Magma chambers with volumes of the order of several tens to several hundred cubic kilometres, as are common, are thus sufficiently large to supply magma to small or moderate eruptions. For large eruptions, however, a much higher percentage of the magma volume must be squeezed out of the chamber. For an ordinary poroelastic chamber, the excess pressure in the chamber falls exponentially during the eruption. For a large eruption to be possible, however, the excess pressure must be essentially maintained until the very end of the eruption. Here I show that caldera collapse can maintain the excess pressure through forced magma-chamber volume reduction, in which case a resulting large eruption would be the consequence (not the cause) of the collapse. I also show that ring-fault dip partly controls the size and intensity (volumetric flow or effusion rate) of the eruption. If the ring-fault dips inward (a normal fault), the displacement is 'stable', the volumetric flow rate (intensity) remains essentially constant during the collapse, and the magma chamber remains active following the collapse. By contrast, if the ring-fault dips outward (a reverse fault) the displacement is 'unstable', the volumetric flow rate normally increases dramatically during the collapse, and the magma chamber may be entirely destroyed during the collapse.

Keywords: volcanoes, magma chambers, collapse calderas, volcanic hazards, ring-dykes, crustal stresses

1. Introduction

Apart from large meteoritic/comet impacts, the only known natural disasters with the potential of having devastating effects on the entire mankind are very large eruptions. It is thus of fundamental importance to understand the processes that give rise to large eruptions. Such an understanding is a necessary condition for forecasting and preparing for such eruptions and, as must ultimately be the goal, to prevent them.

The physical processes that generate small to moderate eruptions are reasonably well understood. The magma chamber ruptures when the internal excess pressure reaches a critical value, normally equal to the in-situ tensile strength of the host rock. Magma flows out of the

chamber, usually up into its roof through a dyke or an inclined sheet. As the magma leaves the chamber, its excess pressure falls exponentially, and so does the volumetric flow or effusion rate through feeder-dyke and associated volcanic fissure. When the excess pressure falls to zero, the magma flow out of the chamber stops, and the eruption comes to an end. While some magma chambers are totally molten, most are partially molten and behave as poroelastic materials (Maaloe and Scheie, 1982; McKenzie, 1984; Gudmundsson, 1987; Marsh, 2000; Sinton and Detrick, 1992; Mutter et al., 1995; MacLeod and Yaouancq, 2000; Singh et al., 2006; Canales et al., 2009). We shall refer to this eruptive process as the ordinary or poroelastic mechanism of eruption.

To squeeze out a large fraction of the magma in a chamber, as is necessary for generating large to very large eruptions (producing tens or hundreds of cubic kilometres of eruptive materials), the ordinary poroelastic mechanism is not sufficient. As indicated, such a mechanism is normally unable to supply more than about 4% of the total volume of magma in the chamber, and usually much less than this percentage. For the poroelastic mechanism to supply magma to a large eruption, an unrealistically large magma chamber would thus be needed. For example, an eruption of 100 km^3 (assuming the feeder-dyke volume is included in this figure) would require a chamber of about 2500 km^3, for felsic magma, and a chamber of 100,000 km^3, for mafic magma. The shapes of collapse calderas are a good indication of the horizontal cross-sectional geometry of the associated shallow magma chamber (Gudmundsson, 1988,2007; Marti et al., 1994, 2008; Marti and Gudmundsson, 2000; Acocella, 2007). Common caldera diameters on Earth are about 10 km, although the largest calderas have maximum diameters of as much as 80 km (Radebaugh et al., 2000; cf. Geyer and Marti, 2008; Gudmundsson, 2008). For a sill-like magma chamber of circular horizontal cross-section and with a diameter of 10 km, the area is 78 km^2. To reach the required volume of 2500 km^3, the chamber thickness would have to be 32 km, which is too large to be plausible. To reach the required chamber volume of 100,000 km^3 for mafic magma, the chamber thickness would have to be 1282 km, which is impossible.

Let us now consider a recent example of a large explosive eruption associated with caldera collapse. The 1815 Tambora eruption in Indonesia produced some 160-170 km^3 of eruptive materials, mainly ash, which is regarded as roughly equivalent to 50 km^3 of magma (Self et al., 1984; Stothers, 1984). The eruption was associated with the formation of a caldera about 6.5 km in diameter. The area of the caldera is thus about 33 km^2. To erupt 50 km^3 of felsic magma by the poroelastic mechanism, the chamber volume would have to be about 1250 km^3. If the horizontal cross-sectional area of the (assumed) sill-like chamber is about 33 km^2, to reach this volume its thickness would have to be about 38 km, a very unlikely figure. The maximum vertical displacement on the ring-fault during the 1815 Tambora eruption is estimated at 1.2 km (Self et al., 1984). The displacement on the ring-fault is thus the most likely reason for squeezing out a large fraction of the magma in the Tambora chamber.

The structure and geometries of collapse calderas has been reviewed in many recent publications (e.g., Munro and Rowland, 1996; Lipman, 1997; Acocella et al., 2003; Aguirre-Diaz et al., 2005; Cole et al., 2005; Holohan et al., 2005; Kusumoto and Takemura, 2005;

Pinel and Jaupart, 2005; Acocella, 2007; Gudmundsson, 2007; Kusumoto and Gudmundsson, 2009; Marti et al., 2009; Geyer and Marti, 2008, 2014) to which the reader is referred for a general overview of collapse calderas, their structures and products. Here the focus is on the mechanical relationship between ring-fault displacements (subsidences) and large eruptions.

A commonly held view is that collapse calderas form, or reactivate (in which case subsidence occurs along an existing ring-fault), as a consequence of magma leaving the chamber, thereby generating a sort of cavity into which the piston-like caldera is supposed to subside. Some similar models, however, assume the fluid pressure in the top of the chamber to be maintained as lithostatic during the collapse (Marti et al., 2000). This mechanism, commonly referred to as the 'underpressure-driven caldera collapse' is discussed and modelled by many; for reviews see Marti et al. (1994), Acocella (2007), and Geyer and Marti (2014). While popular, the underpressure mechanism requires the magma to flow from lower pressure (the underpressured chamber) to higher pressure (the overburden pressure in the host rock), a process that needs to be explained and appears physically implausible.

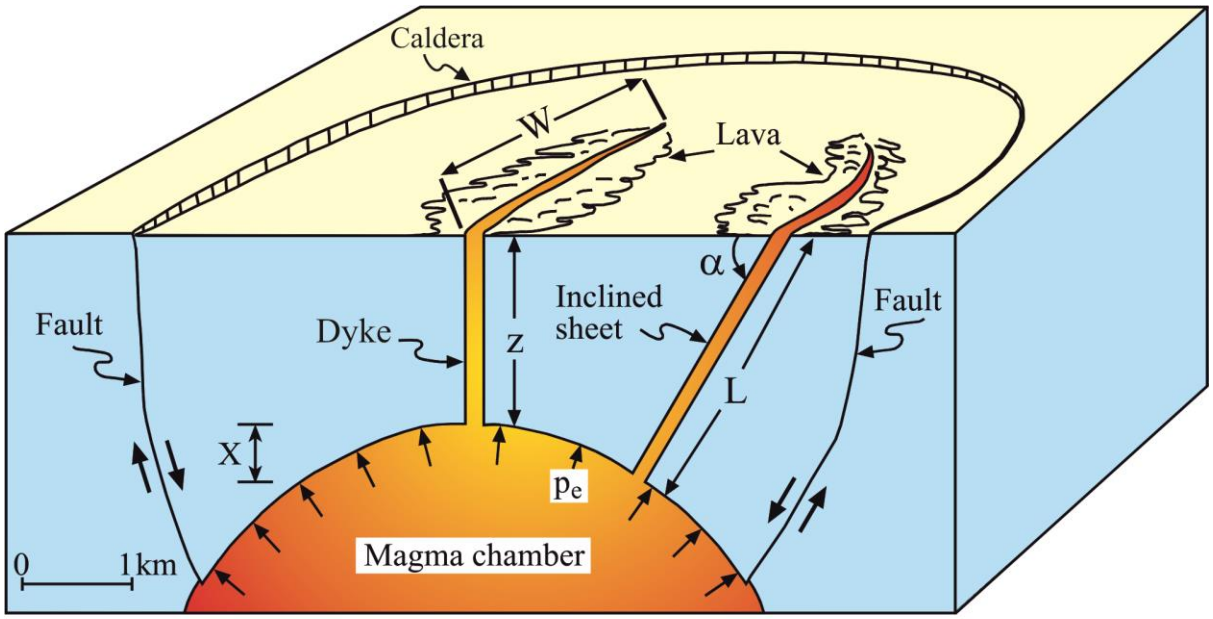

Fig. 1. *Transport of magma to the surface of a polygenetic volcano (here a collapse caldera) is commonly through a vertical dyke or an inclined sheet (Eq. 1). The dyke has the dip dimension z whereas the inclined sheet with the dip α has the dip dimension L. The outcrop length is W (half of which is shown in this cross section). The excess magmatic pressure in the chamber at the time of chamber rupture and dyke/sheet injection is denoted by* p_e. *The difference in the point of initiation of the sheet and the dyke is denoted by x; for a sill-like chamber that difference is normally close to zero.*

During underpressure of a sill-like chamber tensile stress develops in the centre of the roof of the chamber, at its contact with the magma (Pinel and Jaupart, 2005; Gudmundsson, 2007). Such a tensile stress encourages dyke injection into the lower part of the roof. However, the upper part of the roof, close to the surface, is subject to compressive stress, and would thus normally encourages dyke deflection into sill or dyke arrest rather than eruption (Gudmundsson, 2007, 2008). Also, the maximum surface shear stress occurs above the centre

of the chamber, rather than its lateral edges, and therefore does not encourage ring-fault formation. For a spherical circular (spherical) chamber the stress field generate by underpressure is even less likely to encourage the development of a ring-fault (Gudmundsson, 2007). In all underpressure mechanism the caldera collapse is a consequence of the magma flow out of the chamber.

In the present paper, the focus is on a different mechanism, namely one where the caldera subsidence is the cause – not the consequence – of the associated large eruption. More specifically, the ring-fault formation or reactivation is, in this model, related to volcanotectonic processes, in particular to stress concentration due to extension or doming or both of the crustal segment hosting the actual or potential caldera (cf. Gudmundsson, 2007, 2008). The slip on the ring-fault is then largely the result of shear-stress concentration within the zone that hosts the actual or potential fault. Shear-stress concentration is the source drives the slip on all tectonic faults in the Earth's crust, and there is no reason why the source that drives ring-fault slip should be mechanically any different.

The paper also relates the dip of the ring-fault to the volumetric flow of magma or effusion rate of a ring-dyke as a feeder. While most ring-faults are close to vertical, some apparently dip steeply outward as reverse faults while others dip steeply inward as normal faults (e.g., Kusumoto and Takemura, 2005; Acocella, 2007; Gudmundsson, 2007; Kusumoto and Gudmundsson, 2009; Geyer and Marti, 2014; Browning and Gudmundsson, 2015). As the piston-like caldera block subsides along the ring-fault, the opening or aperture of an outward-dipping reverse fault gradually increases, whereas no such increase occurs for an inward-dipping normal fault. Since the volumetric flow rate depends on the cube (the third power) of the aperture of the fracture, the variation in intensity (volumetric flow rate) of a ring-dyke fed eruption should be widely different depending on the dip-direction of the ring-fault.

This paper has two main aims. One is to explain how caldera collapse can maintain the excess pressure in the associated magma chamber during an eruption so as to squeeze out much of, or perhaps all, the magma in the chamber. This is here regarded as one main mechanism for generating large to very large eruptions, and presumably all large explosive eruptions. The second aim is to explore the effects of different dips of the ring-fault on ring-dyke fed volumetric flow rate, that is, eruption intensity.

2. Transport of magma to the surface

Consider a shallow magma chamber (Fig. 1). The chamber may be of any shape; here we show only its semi-circular uppermost part. Generally, however, for collapse calderas to form, sill-like or oblate ellipsoidal chambers are favoured (Fig. 2; Gudmundsson, 2007; Geyer and Marti, 2014). The chamber shown here has two feeders: one is a vertical dyke, the other an inclined sheet - the latter also referred to as a cone sheet. The volcano itself is a collapse caldera (only about half of the caldera is shown in Fig. 1). The shallow chamber is presumably supplied with magma from a deeper reservoir (Fig. 2).

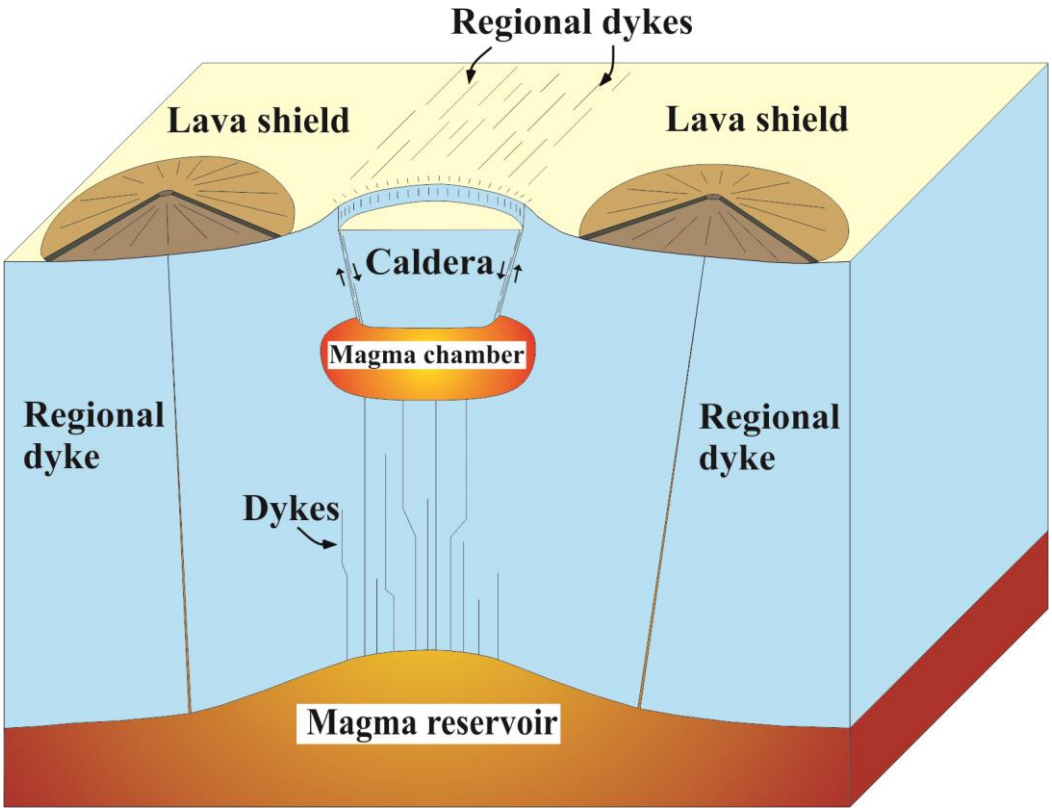

Fig. 2. *Magma can reach the surface either directly from deep-seated reservoirs or from shallow magma chambers which, in turn, are supplied with magma from deep-seated reservoirs. Shallow chambers are the sources of most eruptions in polygenetic volcanoes (here a collapse caldera) which are fed through local dykes and inclined sheets (Fig. 1). Eruptions outside the polygenetic volcanoes are mostly fed by regional dykes, which normally bring to the surface primitive magmas forming lava shields (small shield volcanoes) and other monogenetic basaltic volcanoes.*

When either the vertical dyke or the inclined sheet reaches the surface as a feeder, the volumetric flow rate Q, in m^3s^{-1}, up through the feeder (and issued through a volcanic fissure at the surface) follows from the Navier-Stokes equation for laminar flow between parallel plates (e.g., Lamb, 1932; Milne-Thompson, 1996; Gudmundsson, 2011), namely:

$$Q = \frac{\Delta u^3 W}{12\mu_m}\left[(\rho_r - \rho_m)g\sin\alpha - \frac{\partial p_e}{\partial L}\right] \qquad (1)$$

where Δu denotes the opening or aperture of the feeder-dyke/sheet (or the volcanic fissure at the surface) and W its length or strike dimension of the volcanic fissure at the surface (Fig. 1). Also, μ_m is the dynamic or absolute viscosity of the magma in the dyke/sheet in Pa s, ρ_m is the density of the magma in kg m^{-3} (assumed constant), ρ_r is the average density of the crustal segment (the roof of the magma chamber) through which the feeder propagates to the surface, g is the acceleration due to gravity in m s^{-2}, α is the dip of the feeder in degrees, and $\partial p_e / \partial L$ is the magmatic excess-pressure gradient in the direction of the magma flow, that is, in the direction of the dip dimension L of the feeder in metres (m). For a vertical dyke, the

gradient becomes $\partial p_e / \partial z$. While Eq. (1) is derived for laminar flow and thus most suitable for effusive eruptions, recent results suggest that it also holds, as an approximation, for flows during explosive eruptions (Colucci et al., 2014).

The pressure driving the magma up through the feeder and to the surface derives from two main sources (e.g., Gudmundsson, 2011; Gonnermann and Manga, 2013; cf. Lamb, 1932). One is the excess pressure p_e in the chamber, the other is buoyancy. The excess pressure is the magma pressure in the chamber in excess of the lithostatic pressure. At the time of magma-chamber rupture and dyke/sheet injection (Fig. 1), p_e is normally roughly equal to the in-situ (field) tensile strength of the host rock, generally 0.5-9 MPa, and most commonly about 2-4 MPa (Haimson and Rummel, 1982; Schultz, 1995; Gudmundsson, 2011).

Buoyancy relates to the density difference between the magma and the host rock through which the feeder propagates (Fig. 1) and is represented by the term $(\rho_r - \rho_m)g$ in Eq. (1). Buoyancy is (1) positive when the magma density is less than the density of the host rock, (2) zero when the magma density equals that of the host rock, and (3) negative when magma density is greater than that of the host rock. For basaltic magma injected from shallow magma chambers (Fig. 1), the third situation is common while the first situation applies to almost any magma injected from deep-seated reservoirs and directly to the surface (Fig. 2). Both sources contribute to the general magma overpressure (p_o), also named driving pressure and net pressure, in the feeder. The overpressure or driving pressure is the pressure available to drive the propagation of all sheet-like intrusions, including dykes, inclined sheets, and sills. The overpressure is defined as the total pressure minus the minimum principal compressive stress σ_3 acting on the potential dyke/sheet/sill path before magma emplacement. The reason that σ_3 is the reference principal stress (rather than the maximum σ_1 or intermediate σ_2 principal stresses) is that all sheets are extension fractures and must therefore by definition form in a direction perpendicular to σ_3 (cf. Gudmundsson, 2011). The overpressure may reach several tens of mega-pascals (e.g., Galindo and Gudmundsson, 2012; Becerril et al., 2013) at some points along the path of the feeder (Figs. 1 and 2), although the excess pressure in the source magma chamber is roughly equal to the rock tensile strength and thus typically several mega-pascals (e.g., Gudmundsson, 2011).

One important aspects of Eq. (1) is that the volumetric flow or effusion rate Q during an eruption is proportional to Δu^3. That is, Q depends on the cube of the opening or aperture Δu of the feeder or, at the surface, the volcanic fissure to which the feeder supplies magma. This relation between Q and Δu is referred to as the 'cubic law', particularly in hydrogeology and reservoir science. The relation shows that the effusion rate during a fissure eruption depends much more on the aperture of the fissure than its length. The importance of this law for the intensity of collapse-driven eruptions becomes apparent in Section 5.

3. The poroelastic mechanism of eruption

While some chambers are totally molten, at least during parts of their lifetimes, most crustal chambers are likely to be partially molten and behave as poroelastic bodies (Maaloe and Scheie, 1982; McKenzie, 1984; Gudmundsson, 1987; Marsh, 2000; Sinton and Detrick, 1992; Mutter et al., 1995; MacLeod and Yaouancq, 2000; Singh et al., 2006; Canales et al., 2009). For a partially molten chamber, the rock compressibility (β_r) can be interpreted in terms of the pore compressibility. The total volume of magma V_{er} transported from a totally fluid magma chamber by a feeder-dyke to the surface (including the volume of the feeder itself) during an eruption may be estimated as follows (e.g., Gudmundsson, 1987):

$$V_{er} = \phi p_e (\beta_r + \beta_m) V_t \qquad (2)$$

Here ϕ is the porosity or magma fraction in the chamber (no units), p_e is the magma excess pressure (units of Pa), β_m is the magma compressibility and β_r the rock compressibility (both with units of Pa^{-1}), and V_t is the total volume of the chamber. When the chamber is totally molten, an assumption we will make when calculating the maximum possible eruptive volume of a poroelastic chamber, then β_r is the host-rock compressibility and ϕ = 1. When, however, the chamber is regarded as porous, so that only a fraction ϕ of its total volume is occupied by magma, then β_r is the pore compressibility, which is a measure of the fractional change in pore volume (the volume occupied by magma) during changes in the magmatic excess pressure p_e.

In the poroelastic model, transport of magma out of the chamber and up through the feeder (Figs. 1 and 2) stops and the eruption ends when the excess pressure becomes so small ($p_e \rightarrow 0$) as to be unable to keep the connection between the feeder and the chamber open (particularly for feeders of low-viscosity basaltic magma) at its contact with the chamber (Fig. 1).

3.1 Mafic magma chamber

The fraction of magma in a chamber that is transported out of the chamber during its rupture, feeder-dyke injection, and eruption can now be estimated. From data by Murase and McBirney (1973) the static compressibility β_m for tholeiite (basaltic) magma at 1100-1300ºC is around $1 \times 10^{-10} Pa^{-1}$ (Gudmundsson, 1987; cf. Woods and Huppert, 2003). As indicated above, for a totally molten chamber, ϕ = 1 in Eq. (2) the host-rock compressibility β_r is used in the calculations.

Volatiles affect magma compressibilities. Much of the gas exsolution in mafic magma, however, occurs at very shallow depths, particularly in feeder-dykes when the magma is on its path to the surface. For example, in Hawaii most gas exsolution in basaltic magma occurs

in the uppermost few hundred metres of the feeder/conduit (Greenland et al., 1988). Similarly, studies of mafic dykes worldwide show that most dykes contain only small and rather infrequent vesicles (formed by expanding gas) at depths exceeding several hundred metres below the original surface of the associated volcanic zone/central volcano whereas some feeder-dykes contain numerous and occasionally large vesicles close to the surface (Galindo and Gudmundsson, 2012). Thus, gas exsolution is not likely to have much effect on mafic magma compressibility while the magma is in the chamber.

For a crustal chamber, the host-rock compressibility β_r may be around $2.94 \times 10^{-11}\text{Pa}^{-1}$ if the dynamic/static compressibility ratio is assumed 2.0. For a very shallow magma chamber located in a highly fractured crust, say with a roof at 1-2 km, the dynamic/static ratio may, however, be as high as 10 (Gudmundsson, 2011), in which case the compressibility β_r would be around $1.47 \times 10^{-10}\text{Pa}^{-1}$. Here we use an average of these compressibility estimates, namely a host-rock compressibility of $8.82 \times 10^{-11}\text{Pa}^{-1}$, which should apply to crustal chambers at depths from 1 km to about 5 km. With $\phi = 1$ and using an in-situ tensile strength (assumed equal to p_e) of 4 MPa (Gudmundsson, 2011), Eq. (2) gives the approximate relation between the eruptive volume V_{er} and the total volume of the chamber V_t as:

$$V_{er} \approx 7 \times 10^{-4} V_t \tag{3}$$

This suggests that, although there is considerable range—depending on variation in in-situ tensile strength and host-rock compressibility—typically less than 0.1% (here about 0.07%) of the volume of a totally fluid mafic magma chamber would be erupted/injected during an ordinary poroelastic eruption. If the chamber is less than totally fluid, so that $f < 1$, then this percentage would be even smaller.

3.2 Felsic magma chamber

The overall compressibilities of intermediate magma (Murase and McBirney, 1973) and felsic magma (Kress and Carmichael, 1991; Dobran, 2001) are not much different from that of basaltic magmas. Volatile content, however, affects the magma compressibility (Blake, 1984; Ochs and Lange, 1997; Woods and Huppert, 2003; Malfait et al., 2011; Gao, 2013; Seifert, 2013). Gas is much more compressible than either liquids or solids so that gas bubbles in magma have a much higher compressibility than either the magmatic liquid itself or the solid host rock. The main volatiles in magma are water, H_2O, and carbon dioxide, CO_2, whereas sulphur (as H_2S and SO_2) is also common (e.g., Gonnermann and Manga, 2013). Here the focus is on water and carbon dioxide, the most important volatiles in magma chambers.

It is known that CO_2 exsolves to form bubbles at much greater depths (higher total pressures) than H_2O (Gonnermann and Manga, 2013). CO_2 exsolution and bubble formation occurs in felsic magma (rhyolite) at pressures up to and in excess of 100 MPa, and in basaltic magma at

pressures up to and in excess of 25 MPa. For comparison, using the solubility model of Dixon (1997), Gonnermann and Manga (2013) conclude that H_2O exsolves at total pressures of less than 100 MPa in felsic magma and at 25 MPa in mafic magma. In most volcanic zones 25 MPa corresponds to crustal depth of roughly 1 km depth, and 100 MPa to about 4 km, which is also the depth range of most shallow magma chambers. Thus, for felsic magma in shallow chambers much of CO_2 (and some H_2O) is readily exsolved and forms bubbles. Bubbles in felsic magma have negligible mobility and thus remain within the magma. The only exception is when vigorous convection occurs. Then the gas could accumulate at the top of the felsic magma and form a separate phase. One would thus normally expect the shallow parts of the magma chamber to be more compressible than the deeper parts (cf. Macedonio et al., 2005).

The compressibility of the gas can be $10^{2\text{-}3}$-times greater than the compressibility of the liquid magma (Woods and Huppert, 2003; Malfait et al., 2011; Gao, 2013; Seifert, 2013). Gas bubbles are thus much more compressible than the liquid magma and the associated crystals. The overall compressibility of a mixture of liquid magma and gas, however, depends on the gas fraction in the mixture. When that fraction is small, the compressibility of the liquid magma (β_m) dominates over the compressibility of gas (β_g), to that the compressibility of the mixture is primarily that of the liquid magma. When the gas fraction is large, however, so that the volume fraction of gas in the magma becomes larger than the β_g / β_m ratio then the high compressibility of the gas bubbles increases significantly the overall compressibility of the mixture (Woods and Huppert, 2003). Bubble-rich and highly compressible parts of the magma chamber, where they exist, are likely to be confined to certain layers or compartments (Gudmundsson, 2012) rather than being uniformly distributed. The magma-chamber compressibility may thus be highly heterogeneous, with some compartments being highly compressible and others much less so. The result would be uneven volume changes and overall response of different compartments to volume decrease during eruptions.

Here, however, we are concerned with the general compressibility of the magma in the chamber as a whole. Based on the above considerations, and depending on the amount of felsic magma in the chamber, the compressibility of gas-rich felsic magma (mixture of gas and liquid) could be at least 10 time and possibly 100 times that of a chamber composed entirely of basaltic magma (cf. Woods and Huppert, 2003). For such high magma compressibility, we have $\beta_m >> \beta_r$, in which case Eq. (2) becomes:

$$V_{er} = p_e \beta_m V_t \tag{4}$$

Equation (4), which is commonly used instead of Eq. (2) (Machado, 1974; Blake, 1981; Wadge, 1981), implies that the ratio V_{er} / V_t (ratio of erupted/intruded magma to the total magma volume) depends almost entirely on the magma compressibility β_m. For a purely felsic bubble-rich magma chamber, using p_e = 4 MPa, the ratio is approximately:

$$V_{er} \approx 4 \times 10^{-2} V_t \quad (5)$$

This suggests that as much as 4% of the magma in a felsic chamber (or the bubble-rich felsic compartment of a larger chamber) could leave the chamber (as intrusive and extrusive materials) during chamber rupture and eruption.

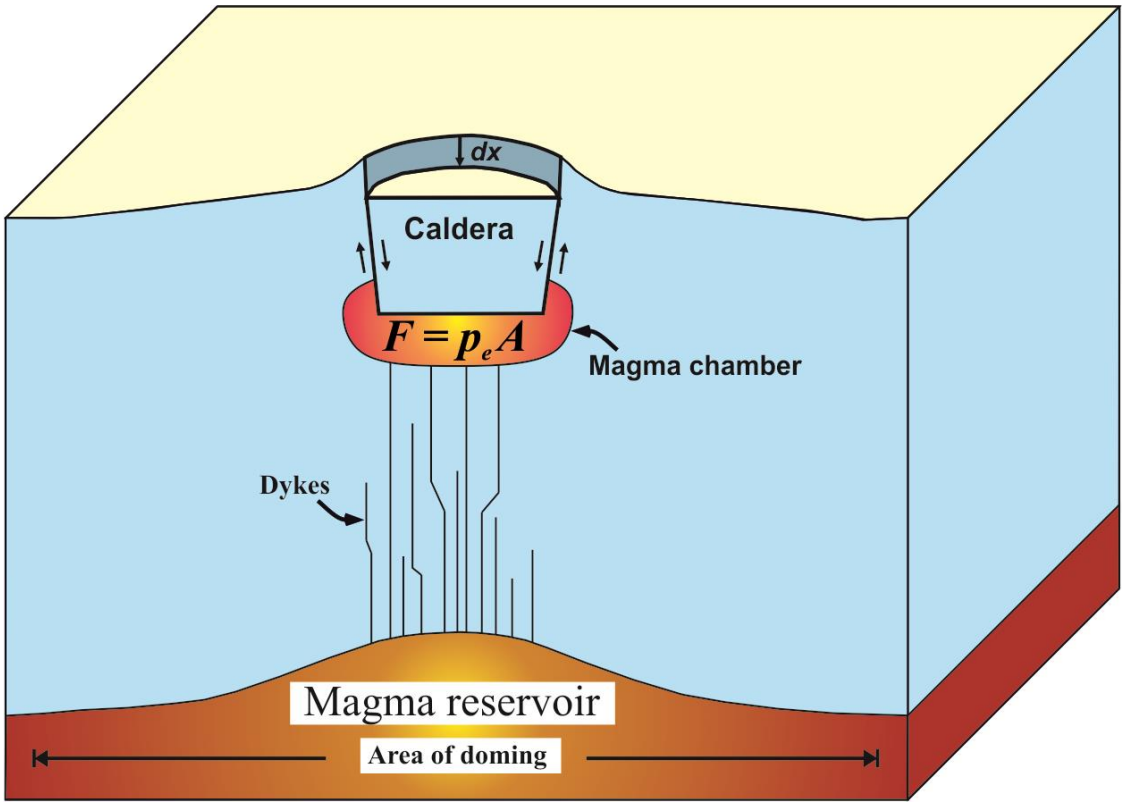

Fig. 3. *When a caldera block subsides (here by the differential distance dx) into the associated magma chamber, the volume of the chamber is reduced (the chamber shrinks) and the excess pressure* p_e *is maintained, thereby allowing much larger fraction of the magma to be squeezed out of the chamber than during an ordinary an poroelastic eruption. The excess pressure* p_e *is related to the average force on the cross-sectional area of the subsiding caldera block A through* $F = p_e A$ *(Eq. 6). For the formation or reactivation of a collapse caldera, an extension or a small uplift or doming of the crustal segment hosting the potential or actual caldera is generally sufficient.*

4. Collapse-driven large eruptions

A moderate or larger volcanic eruption is not a necessary condition for caldera collapse. In four of the five caldera collapses that have been documented instrumentally, little or no eruptions occurred within the caldera. These are (1) the 1912 caldera collapse in Katmai in Alaska (Wood and Kienle, 1992; Hildreth and Fierstein, 2012); (2) the 1968 caldera collapse in Fernandina in the Galapagos (Filson et al., 1973); (3) the 2000 collapse of Myiakejima in Japan (Geshi et al., 2002); and (4) the 2007 collapse of Piton de la Fournaise in Reunion (Fontaine et al., 2014). Only the 1991 collapse of Pinatubo in the Philippines was associated

with a moderate eruption at the site of the caldera, the magma-volume involved being about 4 km^3 (Newhall et al., 1997).

There was magmatism associated with most of the collapses, however. For example, in Katmai there was eruption in Novarupta (a new volcano formed during the eruption) some 10 km from Katmai (Wood and Kienle, 1992; Hildreth and Fierstein, 2012). The volume produced in the eruption, about 30 km^3 (mostly acid and intermediate tephra), was the largest one in the 20^{th} century, the estimated volume of magma leaving the chamber being about 13 km^3. The caldera volume at Katmai, however, is 5-6 km^3, and thus much smaller than the estimated magma volume. Similarly, there were dyke intrusions and small eruptions outside the calderas during the collapses in Myiakejima (Geshi et al., 2002) and Piton de la Fournaise (Fontaine et al., 2014), but none is known in association with the collapse of Fernandina.

In the present model, the reason why moderate or larger eruptions are not needed, and generally not the cause of the collapse, is that the driving energy for the collapse is related to the elastic energy stored in the crustal segment hosting the actual or potential caldera before the collapse (Gudmundsson, 2014). This energy relates partly to doming and/or extension of the crustal segment hosting the shallow chamber and the associated or potential caldera during the unrest period prior to the caldera collapse (Fig. 3). Thus, the elastic energy responsible for the ring-fault initiation, or renewed slip on an existing ring-fault, is primarily related to volcanotectonic processes prior to the collapse. All cavities and holes in solid materials, such as the rocks hosting the magma chamber, concentrate stresses when loaded (Savin, 1961; Gudmundsson, 2011). Magma chambers are cavities that concentrate stresses. These stress concentrations, when of suitable location and magnitude, are the primary reasons for the initiation of a ring-fault (e.g., Gudmundsson, 2007, 2008; Marti et al., 2008; Geyer and Marti, 2014). Once a ring-fault initiates the stress concentration normally increases. This follows partly because any fracture, such as ring-fault, raises or concentrates stresses (Savin, 1961; Gudmundsson, 2011). Partly, however, stress concentrates at the ring-fault once the subsidence begins to form a 'notch' (the caldera), stress concentration being a well-known consequence of notch formation (Savin, 1961). Very small doming – on the scale of centimetres or tens of centimetres - or extension of the crustal segment hosting the potential or actual caldera is commonly enough to cause stress concentration around a shallow (preferably) sill-like magma chamber of a suitable location and magnitude to trigger ring-fault initiation or slip on an existing ring-fault (Gudmundsson, 1998, 2007).

The entire displacement of, say, hundreds of metres, on a ring-fault may be reached in many slips (Filson et al., 1973). The time needed to reach the final displacement, however, varies. For example, the Lake Öskjuvatn collapse in the Askja Central Volcano in Iceland, which began in 1874 apparently, took many years to complete (Hartley and Thordarson, 2012, 2013). Similarly, the total maximum collapse of Myiakejima in Japan in 2000, of about 450 m, took many weeks to complete (Geshi et al., 2002). The maximum displacement of 350 m during the collapse of Fernandina in Galapagos in 1968 happened quickly, but occurred in some 75 individual slips, each of which being 4-5 m (Filson et al., 1973).

In the model presented here, there are two main processes for generating large eruptions during caldera collapse. One is the reduction in the chamber volume as the piston-like caldera block subsides into the chamber (Fig. 3). This mechanism is the general one, and is discussed below. The other mechanism applies primarily to gas-rich magmas, and thus to felsic chambers, and relates to individual slips on the ring-fault generating overpressure through gas

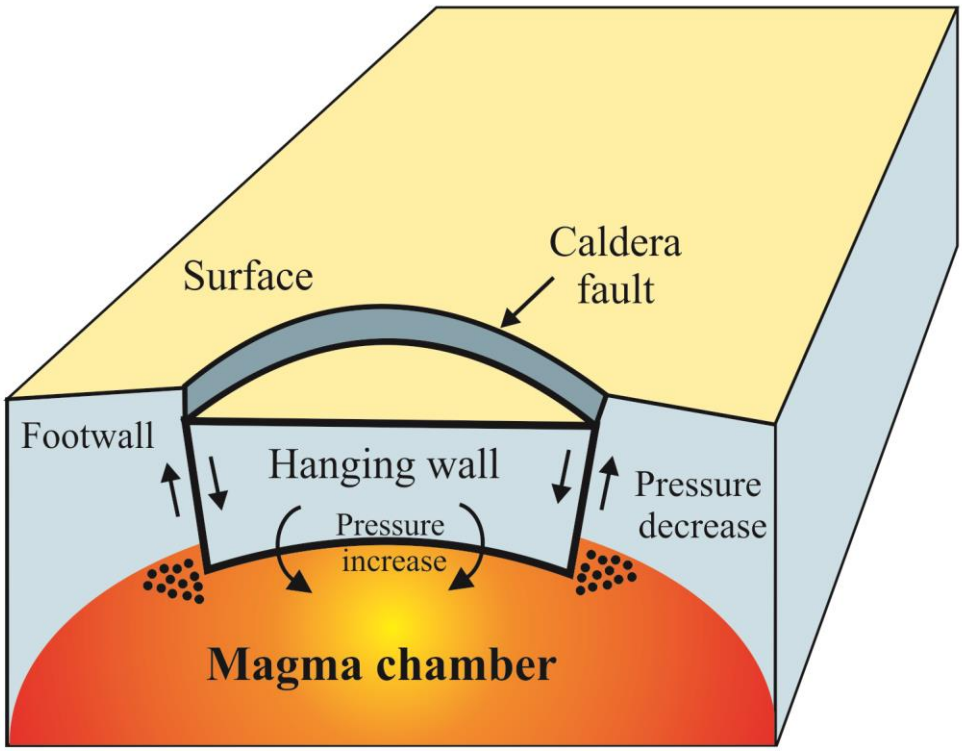

Fig. 4. *During slip on an inward-dipping normal ring-fault, the flanks (the hanging wall of the ring-fault) rise as the central block subsides. The associated decrease in vertical stress or geostatic pressure on a gas-rich magma beneath the flanks may give rise to rapid gas exsolution in those parts of the magma chamber. Multiple slips on the ring-fault and repeated gas exsolution during the collapse would help maintain the excess pressure in the chamber, thereby making it possible to squeeze out larger fraction of the magma in the chamber than would be possible during an ordinary poroelastic eruption of the chamber.*

exsolution (Fig. 4). This latter mechanism may apply to ring-faults in general, but is likely to be particularly effective during slip on normal-fault calderas (Gudmundsson, 1998). As the block inside the ring-fault subsides, commonly in many slip events, the flanks rise in the same events. This follows because the vertical stress on the flanks just outside the ring fault decreases, and thus decreases on the magma beneath the flanks (at the same time as it increases on the magma below the piston-like subsiding block). An absolute rise of the flanks of grabens during subsidence of the graben floor has, for example, be measured during rifting episodes in Iceland and Hawaii (Pollard et al., 1983). The repeated pressure decrease below the flank areas during slips encourages gas exsolution form gas-rich magma (Fig. 4), and thus the build-up and maintenance of the excess pressure in the flank-parts or compartments of the magma chamber (Gudmundsson, 1998). Since these compartments are also those right below

and close to the ring-fault, their excess pressure will also encourage the injection of a ring-dyke, as discussed further below.

The other mechanism for the maintenance of the excess pressure in the chamber, and thus the primary reason for squeezing magma out of the chamber during caldera collapse, is the volume reduction or shrinkage of the chamber as the piston-like block subsides (Fig. 2). The mechanism can be summarised as follows (Fig. 3). The force moving the piston-like caldera floor down into the chamber is equal to the excess pressure times the cross-sectional area of the caldera *A*, that is (e.g., Callen, 1985; Kondepudi, 2008):

$$F = p_e A \tag{6}$$

Let the piston-like caldera roof move the differential distance *dx* (Fig. 3). Then the corresponding infinitesimal work *dW* done by the surrounding crustal segment (the host rock) on the magma chamber system is:

$$dW = Fdx = p_e A dx \tag{7}$$

At the same time the volume of the chamber changes by dV_c , given as:

$$-dV_c = Adx \tag{8}$$

We use a minus sign in Eq. (8) because the chamber volume decreases during the piston-like caldera subsidence. We follow the thermodynamic convention that work done on a thermodynamic system, here the chamber, is considered positive. Using Eqs. (6) and (7) and the relation $dW = dU$ (the first law of thermodynamics when no heat is added to the system), where *dU* is the change in internal energy of the magma chamber during its volume reduction or shrinkage, we have:

$$dU = -p_e dV_c \tag{9}$$

which gives the elastic potential energy *dU* transformed or released during caldera subsidence as a function of the excess pressure p_e and the contraction or shrinkage of the chamber dV_c.

We know that the excess pressure p_e at the time of magma-chamber rupture and feeder-dyke injection is roughly equal to the in situ tensile host-rock strength, T_0. The tensile strength, in turn, is almost a constant, mostly 1-6 MPa and typically around 4 MPa (Gudmundsson, 2011). Thus, the excess pressure p_e at the time of chamber rupture is essentially constant, here taken as 4 MPa. In the present model of collapse-driven large eruptions, it is this pressure which is maintained until close to the end of the eruption. From Eq. (9) it then follows that the elastic potential energy of the eruption is directly related to the contraction or shrinkage of the chamber during the caldera subsidence and eruption, that is, dV_c, which corresponds roughly to the volume of magma (or mixture of magma and gas) which leaves the chamber

during the eruption. For shallow magma chambers, feeder-dyke volumes are normally fraction of a cubic kilometre, and maximum several cubic kilometres. For large eruptions of the orders of tens or hundreds of cubic kilometres or more (calculated as magma) the feeder-dyke volume may be regarded as being included in the estimated eruptive volume V_{er}. From these considerations it follows that we can identify V_{er} with $-dV_c$ to obtain the elastic potential energy U_{er} driving the caldera-forming eruption from the following equation:

$$U_{er} = p_e V_{er} \tag{10}$$

It is this potential energy which is the main mechanism (while gas exsolution helps, particularly for gas-rich magmas) that drives the magma out during large collapse-generated eruptions.

5. Effect of the ring-fault dip on the eruption intensity

5.1 Formation of a ring-fault

Caldera collapses occur along ring-faults, all of which are primarily dip-slip faults. The ring-faults are primarily shear fractures, but some become injected by magma to form ring-dykes, and then mixed-mode (shear and extension) fractures. For ring-faults to form there must be suitable stress concentration above the margins of the associated shallow magma chamber. This concentration happens only rarely, as indicated by caldera collapses being rare in comparison with the number of dyke injections and eruptions in the volcano. The condition for ring-fault formation or slip can be expressed by the Coulomb criterion, namely (e.g., Jaeger and Cook, 1979; Gudmundsson, 2011):

$$\tau = \tau_0 + \mu\sigma_n \tag{11}$$

Here τ is the driving shear stress on the ring-fault plane, τ_0 is the cohesive or inherent shear strength of the rock, μ is the coefficient of internal friction, and σ_n is the normal stress on the fault plane. The (inherent) shear strength of the material is its shear strength when no normal stress is applied. In rock physics, the criterion is commonly written in the form:

$$\tau = 2T_0 + \mu\sigma_n \tag{12}$$

referred to as the modified Griffith criterion and derives from the Griffith theory of brittle failure (Gudmundsson, 2011). Here the shear strength is substituted with twice the tensile strength, that is, $\tau_0 = 2T_0$, which is in agreement with measurements.

Equations (11) and (12) are for dry rocks, whereas all rocks below a certain (normally shallow) crustal depth contain fluids, mostly water, referred to as pore fluids. Increasing the pore-fluid pressure, as is common in volcanoes during deformation, particularly those that

contain geothermal fields, increases the likelihood of fault initiation or slip for all types of faults, including ring-faults. In addition the pore-fluid pressure, there may be fluids under pressure on the potential or actual ring-fault plane itself. The fluids may be groundwater, volcanic gas, geothermal water, and magma (forming a ring-dyke). When any such fluids are present on the ring-fault plane, Eqs. (11) and (12) become (e.g., Gudmundsson, 2011):

$$\tau = \tau_0 + \mu(\sigma_n - p_t) \tag{13}$$

$$\tau = 2T_0 + \mu(\sigma_n - p_t) \tag{14}$$

Here p_t is total fluid pressure on the ring-fault plane at the time of fault initiation or slip. Eqs. (13) and (14) imply as follows for ring-faults:

- When the total fluid pressure p_t equals the normal stress σ_n the term $\mu(\sigma_n - p_t)$ becomes zero and the driving shear stress for slip becomes τ_0, which is equal to $2T_0$. For magma forming a ring-dyke, p_t is in fact higher than σ_n because of the magmatic overpressure that drives the dyke up the ring-fault.
- Since the in situ tensile strength of rocks is typically in the range of 1-6 MPa and mostly about 2-4 MPa, it follows that the typical driving shear stress for slip on the ring-fault (and fluid-pressured faults in general) is commonly 4-8 MPa, in agreement with common stress drops (Kanamori and Anderson, 1975).
- Fault slip is greatly facilitated when $\mu(\sigma_n - p_t)$ equals zero or becomes negative. Not only because the normal stress σ_n on the fault plane becomes zero or negative (negative if a ring-dyke forms), but also because the friction along the fault plane is very much reduced. That is, the fluid (water, magma, gas) lubricates the fault plane and makes displacement easier.

A ring-dyke is not a necessary condition for a ring-fault to form or slip, but such a dyke makes slip much easier and decreases the chance that the propagating ring-fault becomes arrested (Fig. 5). In fact, no ring-dyke apparently formed in four of the five main caldera collapses instrumentally recorded during the past century, that is, in Katmai (1912), Fernandina (1968), in Myiakejima (2000), and in Piton de la Fournaise (2007). A ring-dyke may, however, have formed in Pinatubo (1991). Nevertheless, if a ring-dyke is emplaced, it becomes more likely that a comparatively large caldera collapse will occur. Most ring-faults are steeply dipping, many dipping close to vertical (Figs. 1-3). The reason why ring-faults do not have ordinary dip-slip fault dips of 50-70º is that the stress concentration around the associated shallow chamber modifies the stress field so as to favour close-to-vertical dip-slip faults (Gudmundsson, 1998). More specifically, the maximum principal compressive stress σ_1 dips in such a way that if the fault makes the angle of, say 30º to σ_1 then the ring-fault would be very close to vertical.

During some caldera collapses, however, part of the ring-fault does not slip at all. Examples include trapdoor collapses, such as have been observed in the calderas of the Galapagos

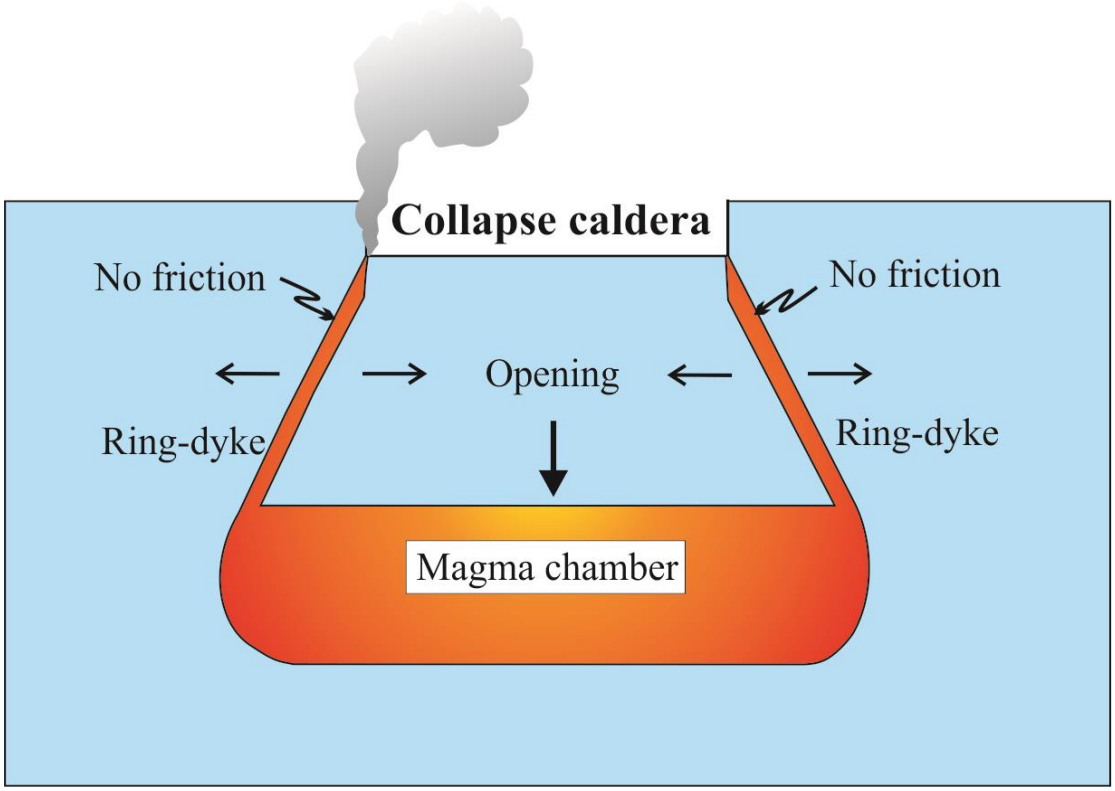

Fig. 5. *During caldera subsidence (vertical arrow) on an outward-dipping reverse ring-fault, the ring-fault must open up (indicated by horizontal arrows). It follows that the fault would normally be injected by a ring-dyke which is likely to reach the surface and supply magma to an eruption. Because of the ring-dyke, there is essentially no friction along the ring-fault and the caldera block may subside to the bottom of the chamber. The ring-fault displacement is thus unstable. The main mechanical implications are (1) that the volumetric flow or effusion rate should increase greatly with increasing subsidence of the caldera block, and (2) most or all the magma in the chamber may be squeezed out during the eruption. Thus, the eruption may be very large and the chamber all but destroyed during the collapse.*

Islands (Amelung et al., 2000). Normally, however, most of, or the entire, ring-fault is involved in the collapse.

5.2 Effects of ring-fault dip on the eruption

While a ring-dyke is not needed for caldera collapses to occur, such a dyke would almost always be injected during collapse along outward-dipping faults, that is, reverse faults (Fig. 5). This follows because the geometric consequence of the outward-dipping ring-fault is theoretically an open cavity, an open ring-fault which reaches down to the magma chamber itself. As the piston-like caldera block subsides, the opening of the ring-fault increases (Figs. 5 and 6). Magma in the chamber tends to flow to open cavities or faults which are, technically, regions of lowered potential energy. Thus, magma would tend to flow into the gradually opened fault to form a ring-dyke.

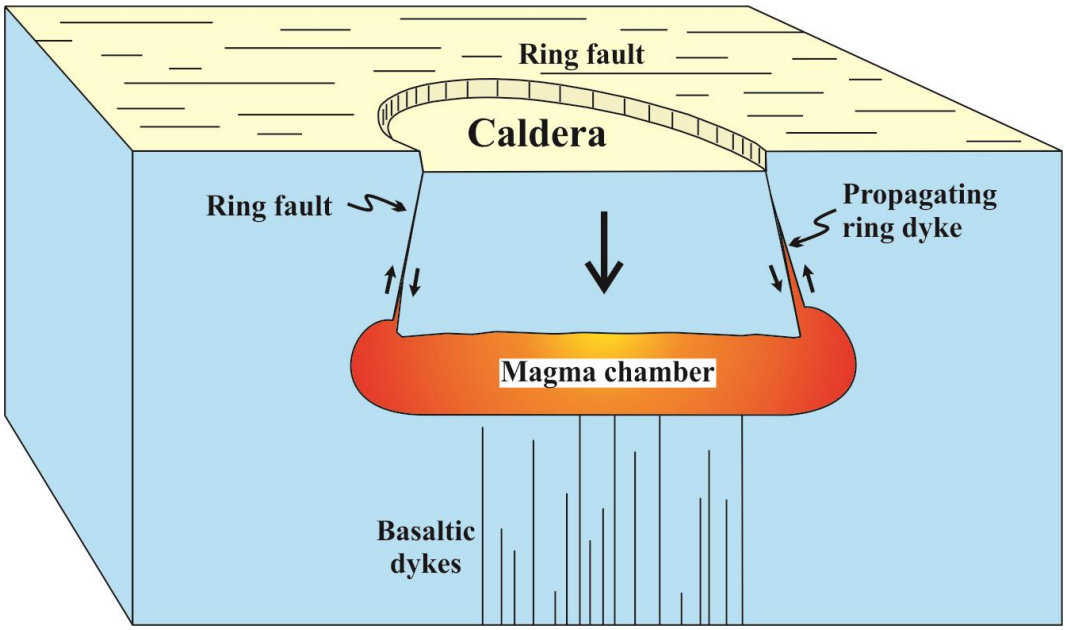

Fig. 6. *Schematic illustration of the early stages of ring-dyke emplacement along an outward-dipping reverse ring-fault. As the caldera block subsides, the ring-fault opens more and more, hence the ring-dyke becomes thicker until, eventually, the ring-dyke reaches the surface (Fig. 5). Here the ring-dyke has propagated into part of the ring-fault, but as the subsidence continues the dyke will, eventually, occupy much of, or the entire, ring-fault. The ring-fault slip is here unstable.*

The existing evidence for outward-dipping versus inward-dipping ring-faults has been widely discussed (Gudmundsson, 1998, 2008; Cole et al., 2005; Acocella, 2007; Kusumoto and Gudmundsson, 2009; Geyer and Marti, 2014; Browning and Gudmundsson, 2015), and the details will not be repeated here. Here we merely state that there is some field evidence for both types of ring-faults, that is, inward dipping and outward dipping. The main point is that ring-fault dips have implications for the collapse mechanisms and the associated eruptions. We shall now consider these implications, starting with the outward-dipping or revers ring-faults. Thus, for an *outward-dipping ring-fault* extending to the surface the main points are as follows:

1. The volumetric flow rate Q supplied by the ring-dyke feeding a surface eruption should increase with increasing subsidence of the caldera floor. As the piston-like caldera block subsides into the magma chamber, the opening or aperture of the fracture between the host rock and the block gradually increases (Figs. 5 and 6). Since Q is related to the ring-dyke aperture or opening Δu in the third power (Eq. 1), the aperture increase with caldera subsidence along an outward-dipping ring-fault should result in a very great increase in the volumetric flow rate during the subsidence.

2. Given the geometric configuration and, in particular, the gradual opening or aperture increase of the ring-fault during the caldera subsidence, it is likely that any outward-

dipping ring-fault will be injected by a ring-dyke (Figs. 5 and 6). More specifically, an outward-dipping ring-fault would normally supply magma to the surface (through a ring-dyke). Thus, non-eruptive ring-faults are unlikely to be outward-dipping reverse faults; they are most likely to be inward-dipping normal faults.

3. Because of the injected magma to form the ring-dyke there will be essentially no friction along the ring-fault (Figs. 5 and 6), only the viscosity effects of the magma that forms the ring-dyke. As the ring-dyke opening increases with increasing caldera-block subsidence on the outward-dipping fault, there is theoretically nothing to stop the piston-like block from sinking to the bottom of the chamber (Figs. 5 and 6). The consequence is for an outward-dipping ring-fault, a ring-dyke should form, and close to the entire magma chamber could erupt. This applies to a totally molten chamber made of a single compartment, but even for more complex magma chambers (Gudmundsson, 2012), slip on an outward-dipping ring-fault implies that a very large fraction of the magma in the chamber becomes erupted through the ring-dyke. Consequently, little if any magma should be left in the chamber following collapse on an outward-dipping ring-fault. By analogy with fracture propagation, such a caldera collapse can be referred to as unstable.

The other basic model of ring-fault attitude is the inward-dipping or normal fault (Figs. 1-3). Inward-dipping ring-faults tend to form when the crustal segment containing the volcano and its shallow chamber is subject to extension or doming (Fig. 3). Such a stress field occurs in all volcanoes related to rift zones, such as at divergent plate boundaries and in continental grabens, and also where the volcanic field or zone containing the volcano is subject to doming. Extension sufficient for inward-dipping ring-fault to form can be generated through cm-scale or tens-of-cm scale doming induced by a deeper reservoir (Fig. 3; Gudmundsson, 2007), rift-related extension, gravity sliding resulting in volcano spreading, and other similar mechanisms. For the mechanism of inward-dipping ring-faults extending to the surface, there are several points to consider, namely the following:

1. Unless a ring-dyke forms, there is always friction along the inward-dipping fault (Fig. 7), which is one reason why the slip is more controlled than in the case of an outward-dipping ring fault. Partly because the shallow magma chamber acts as a cavity that raises stress, and partly because of the developing or slipping (existing) ring-fault itself, tensile stresses concentrate in and around the piston-like caldera block. This tensile stress may then reduce friction along the ring-fault and promote caldera subsidence.

2. If the inward-dipping ring-fault is close to vertical, is injected by a ring-dyke, or both, then a total collapse is possible. This implies, as in the case of the outward-dipping ring-fault, that the magma chamber may be, to a large degree, emptied during the eruption. For other conditions, the friction on inward-dipping ring-faults limits the subsidence to a maximum of, in most cases, a few hundred metres and, occasionally, 1-2 km.

3. On parts of a ring-fault where there is high friction, such as parts where no ring-dyke forms (Fig. 7), or parts where the dip of the ring-fault is unusually gentle and the normal stress high, there may be little or no fault slip during the collapse. These are presumably the main reasons for the formation of trap-door calderas. Thus, for inward-dipping ring faults, the slips are more controlled than for outward-dipping faults. By analogy with fracture propagation, we refer to caldera collapse on inward-dipping faults as stable.

We thus conclude that slip on inward-dipping ring-faults is likely to be generally stable or controlled, whereas that on outward-dipping ring-faults is unstable. The considerations above suggest that, as a rule, outward-dipping ring faults should be occupied with a ring-dyke that acts as a feeder for a part, or the entire, caldera-forming eruption. More specifically, given the geometric relationships (Fig. 5), an eruption fed by an outward-dipping ring-dyke should normally increase its volumetric flow rate greatly during the caldera subsidence. That is, the intensity of the eruption should be positively related to the subsidence or vertical displacement. Also, for an outward-dipping ring-fault, a large part, or the whole, of the magma chamber should normally become emptied; that is, the magma chamber may be expected to be destroyed in the eruption. None of these conclusions apply generally to inward-dipping ring-fault faults whose displacement is normally stable, whose magma chambers are normally expected to survive the eruption, and whose ring-dyke fed eruption intensity is likely to be stable during much of the eruption.

6. Discussion and conclusions

Understanding the processes that give rise to large eruptions is of fundamental importance in theoretical and applied volcanology. Eruptions that produce hundreds or thousands of cubic kilometres of eruptive materials are very rare. Yet, they occur at intervals of tens of thousands of years or less, and most certainly pose a threat to mankind on a scale that very few other natural hazards do. In order to assess the potential of such eruptions worldwide we must first understand the physical processes that give rise to such eruptions. One principal aim of the present paper is to advance our understanding of the likely processes. Once that understanding is on board, we can move to the next step – which is to mitigate large eruptions; or, more specially, to prevent them through releasing the energy available for large eruptions in many small steps. That topic, however, will be treated elsewhere.

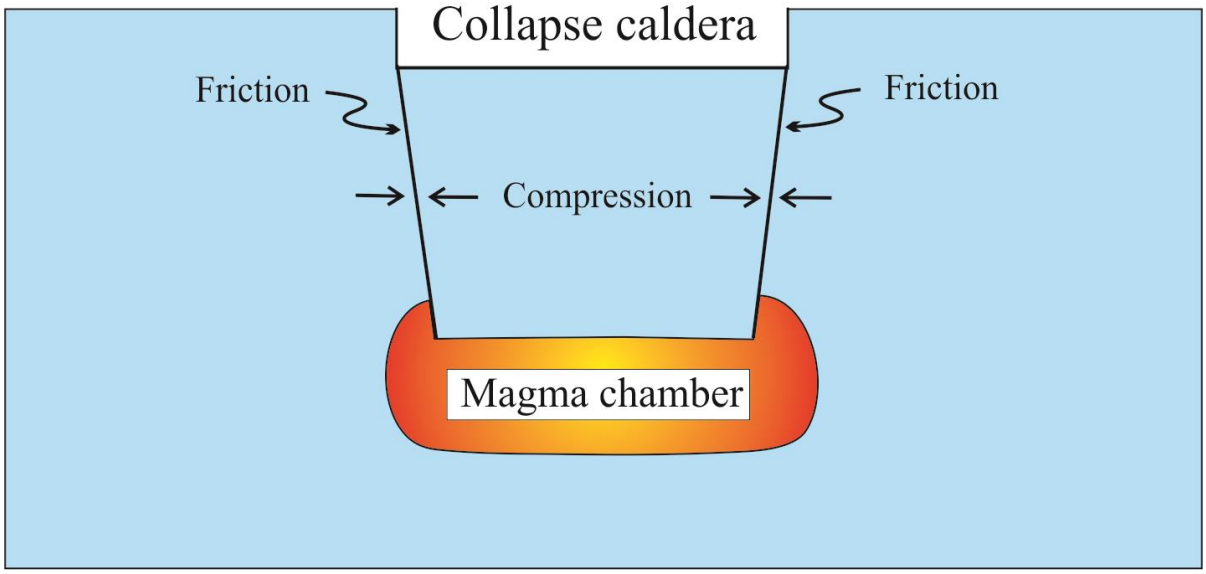

Fig. 7. *Schematic illustration of caldera subsidence on an inward-dipping normal ring-fault. As the caldera block subsides, it becomes subject to higher horizontal compression (compressive stress). So long as no ring-dyke is injected along the fault, the friction together with the normal stress on the ring-fault ensure that the fault remains closed and the displacement stable. Thus, collapse on an inward-dipping normal ring-fault is less likely than an outward-dipping ring-fault to result in increasing volumetric flow rate (Eq. 1) through a ring-dyke as the subsidence increases. Also, the magma chamber is here unlikely to be destroyed during the collapse.*

Here the focus is on the relation between caldera collapses and large eruptions. In the model presented here a large eruption is the consequence—not the cause—of the collapse. This mechanism may thus be referred to as 'caldera-collapse driven eruptions' or 'collapse-driven eruptions' for short. The essential idea is that as the caldera block subsides it automatically reduces the volume of the magma chamber (Figs. 2 and 3). As a consequence the magmatic excess pressure (Eq. 1) is maintained in the chamber for much longer time than during ordinary poroelastic (non-collapse) eruptions. It follows that a much larger fraction of the magma in the chamber can be squeezed out during the eruption, hence a large eruption. Given that magma chambers are commonly 50-500 km^3, and some much larger, the caldera-collapse mechanism is able to explain large to very large eruptions from magma chambers that normally give rise to small to moderate eruptions through the ordinary poroelastic mechanism.

The potential for caldera-driven large eruptions is further enhanced through the ring-fault generating pressure changes in the magma. This applies particularly to gas-rich magmas where the ring-fault is an inward-dipping normal fault (Fig. 4). During each slip, much of the displacement is a downward movement of the piston-like caldera block (the hanging-wall part), but there will also be some rise of the flanks, that is, the footwall parts. This rise temporarily decreases the vertical stress on the magma beneath the footwall and thus encourages gas exsolution and, thereby, further maintenance of the excess pressure in the chamber. Thus, the general shrinkage of the chamber volume as well as repeated small-scale rise of the flanks of the footwall of the ring-fault together maintain the excess pressure in the

chamber long enough to squeeze out a large fraction of—and occasionally essentially all—the magma in the chamber.

The dip of the ring-fault should, theoretically, have great effects on the style and volumetric flow (effusion) rate during a ring-dyke fed eruption. It follows from the geometric considerations in Fig. 7 that the opening or aperture of the ring-fault should increase with increasing vertical displacement or caldera subsidence on an outward-dipping fault. When the fault aperture or opening increases the volumetric flow or effusion rate of caldera eruption fed by a ring-dyke should greatly increase (Eq. 1). This follows because the volumetric flow rate increases with the aperture in the third power (the cubic law).

At present, we do not really have good data to test these theoretical conclusions. First, there is not sufficient data to demonstrate whether the effusion rate increases as the caldera-block subsides. Second, we do not know whether caldera eruptions are primarily supplied with magma through ring-dykes or are central-conduit fed. Some caldera-forming eruptions are partly along a ring-dyke, while others appear to be primarily in the central part of the caldera. The central part may then either be the main conduit of a stratovolcano that subsequently collapses or from the central part of an already existing caldera. Also, many collapses, particularly in basaltic edifices, occur with little or no eruptions.

The outward-dipping ring-fault model implies that many magma chambers are largely or even totally destroyed during the collapse—that a large fraction or effectively all the magma is squeezed out of the chamber. Observations suggest that some magma chambers are destroyed by caldera collapses, with little if any volcanic activity within a given caldera following a major collapse (e.g., Marti and Gudmundsson, 2000; Marti et al., 2000). Many calderas, however, appear to be are highly active after collapse (Newhall and Dzurisin, 1988). For example, there have been eruptions in Fernandina (following the 1968 collapse), in Pinatubo (following the 1991 collapse), in Miyakejima (following the 2000 collapse), and in Piton de la Fournaise (following the 2007 collapse). Since these eruptions occur so shortly after the collapses (before a new chamber would have time to form) they indicate that the associated magma chambers were not destroyed during the collapse.

In conclusion, the present model provides one explanation for the generation of large—particularly explosive—eruptions. The model also explains the well-known association of large explosive eruptions with caldera collapses. Furthermore, the model offers clear mechanisms whereby the magmatic excess pressure can be maintained for essentially the entire duration of the eruption, thereby explaining how magma chambers of typical sizes that generally produce small to moderate eruptions can occasionally produce large to very large explosive eruptions.

The mechanisms suggested here distinguish between inward-dipping normal ring-faults and outward-dipping reverse ring-faults. While slips on inward-dipping faults are ‘stable’ and may yield no or comparatively small eruptions, even from large chambers, slips on outward-dipping reverse ring-faults are ‘unstable’. That means that there is hardly anything to stop the

subsidence of the crustal block bounded by an outward-dipping ring fault once the subsidence has started. Thus,. they tend to squeeze out a very large part of or the entire volume of magma in the chamber. Furthermore, because the opening or aperture of an outward-dipping ring-fault increases as the subsidence progresses, the volumetric flow rate from a feeder-ring dyke should increase greatly during the subsidence. Eruptions associated with outward-dipping ring-faults would thus normally be very intense and commonly destroy the magma chamber, while neither of these predictions necessarily apply to eruptions associated with inward-dipping ring-faults. It remains to be seen whether these predictions are borne out by observations.

Acknowledgements

I thank Nahid Mohajeri for help in preparing this paper. I also thank the Editor, Joan Marti, and the reviewers, Adelina Geyer and Marco Neri, for very helpful comments.

References

Acocella, V., 2007. Understanding caldera structure and development: and overview of analogue models compared to natural calderas. Earth-Science Reviews, 85, 125-160.

Acocella, V., Korme, T., Salvini, F., Funiciello, R., 2003. Elliptic calderas in the Ethiopian Rift: control of pre-existing structures. Journal of Volcanology and Geothermal Research, 119, 189-203.

Aguirre-Diaz, G.J., Labarthe-Hernandez, G., Tristan-Gonzalez, M., Nieto-Obregon, J., 2005. Graben-calderas of the Sierra Madre Occidental, Mexico. In: J. Marti and J. Gottsmann (eds.), Caldera Volcanism: Analysis, Modelling and Response. Workshop, Tenerife, Spain, p. 6.

Amelung, F., Jonsson, S., Zebker, H., Segall, P., 2000. Widespread uplift and `trapdoor' faulting on Galapagos volcanoes observed with radar interferometry. Nature, 407, 993-996.

Becerril, L., Galindo, I., Gudmundsson, A., Morales, J.M., 2013. Depth of origin of magma in eruptions. Scientific Reports 3, 2762. doi: 10.1038/srep02762

Blake, S., 1981. Volcanism and the dynamics of open magma chambers. Nature, 289, 783-785.

Blake, S., 1984 Volatile oversaturation during the evolution of silicic magma chambers as an eruption trigger. Journal of Geophysical Research, 89, 8237– 8244.

Browning, J., Gudmundsson, A., 2015. Caldera faults capture and deflect inclined sheets: An alternative mechanism of ring-dike formation. Bulletin of Volcanology, 77, 889, doi: 10.1007/s00445-014-0889-4.

Callen, H.B., 1985. Thermodynamics and an Introduction to Thermostatics, 2nd ed. Wiley, New York.

Canales, J.P., Nedimovic, M.R., Kent, G.M., Carbotte, S.M., Detrick, R.S., 2009. Seismic reflection images of a near-axis melt sill within the lower crust at the Juan de Fuca ridge. Nature, 460, 89-93.

Colucci S., de'Michieli Vitturi, M., Neri, A., Palladino, D., 2014. An integrated model of magma chamber, conduit, and column for the analysis of sustained magmatic eruptions, Earth and Planetary Science Letters, 404, 98-110.

Cole, J.W., Milner, D.M., Spinks, K.D. 2005. Calderas and caldera structures: a review. Earth Science Review, 69, 1-26.

Dixon, J.E., 1997. Degassing of alkali basalts. American Mineralogist, 82, 368-378.

Dobran, F., 2001. Volcanic Processes: Mechanisms in Material Transport. Springer Verlag, Berlin.

Filson, J., Simkin, T., Leu, L. 1973. Seismicity of a caldera collapse: Galapagos Islands 1968. Journal of Geophysical Research, 78, 8591-8622.

Fontaine, F.R., Roult, G., Michon, L., Barruo, G., Di Muro, A., 2014. The 2007 eruptions and caldera collapse of the Piton de la Fournaise volcano (La Reunion Island) from tilt analysis at a single very broadband seismic station. Geophysical Research Letters, 41, 2803-2811, doi:10.1002.grl.v.41.8.

Galindo, I., Gudmundsson, A., 2012 Basaltic feeder dykes in rift zones: geometry, emplacement, and effusion rates. Natural Hazards and Earth System Sciences, 12, 3683–3700.

Geshi, N., Shimano, T., Chiba, T., Nakada, S. 2002. Caldera collapse during the 2000 eruption of Miyakejima Volcano, Japan. Bulletin of Volcanology, 64, 55-58.

Geyer, A., Marti, J., 2008. The new worldwide collapse caldera database (CCDB): A tool for studying and understanding caldera processes. Journal of Volcanology and Geothermal Research, 175, 334-354

Geyer, A., Marti, J., 2014. A short review of our current understanding of the development of ring faults during collapse caldera formation. Frontiers in Earth Science, 2: 22. doi:10.3389/feart.2014.00022.

Gonnermann, H.M., Manga, M., 2013. Dynamics of magma ascent in the volcanic conduit. In: Fagents, S.A., Gregg, T.K.P., Lopes, R.M.C. (eds), Modeling Volcanic Processes. Cambridge University Press, Cambridge, pp. 55-84.

Greenland, L. P., Okamura, A. T., Stokes, J. B., 1988. Constraints on the mechanics of the eruption. In: Wolfe, E. W (ed), The Puu Oo Eurption of Kilauea Volcano, Hawaii: Episodes Through 20, January 3, 1983 Through June 8, 1984, US Geol. Survey Professional Papere, 1463, 155–164.

Gudmundsson, A., 1987. Formation and mechanics of magma reservoirs in Iceland. Geophysical Journal of the Royal Astronomical Society, 91, 27-41.

Gudmundsson, A., 1988. Formation of collapse calderas. Geology, 16, 808-810.

Gudmundsson, A. 1998. Formation and development of normal-fault calderas and the initiation of large explosive eruptions. Bulletin of Volcanology, 60, 160-170.

Gudmundsson, A., 2007. Conceptual and numerical models of ring-fault formation. Journal of Volcanology and Geothermal Research, 164, 142-160.

Gudmundsson, A., 2008. Magma-chamber geometry, fluid transport, local stresses, and rock behaviour during collapse-caldera formation. In: Gottsmann, J., Marti, J. (eds.), Caldera Volcanism: Analysis, Modelling and Response. Developments in Volcanology 10. Elsevier, Amsterdam, pp. 313-349.

Gudmundsson, A., 2011. Rock Fractures in Geological Processes. Cambridge, Cambridge University Press.

Gudmundsson, A., 2012. Magma chambers: formation, local stresses, excess pressures, and compartments. Journal of Volcanology and Geothermal Research, 237-238, 19–41.

Gudmundsson, A., 2014. Energy release in great earthquakes and eruptions. Frontiers in Earth Science 2:10. doi: 10.3389/feart.2014.00010

Guo, X., 2013. Density and Compressibility of FeO-bearing Silicate Melt: Relevance to Magma Behavior in the Earth. PhD Thesis, University of Michigan, Ann Arbor, Michigan.

Haimson, B.C., Rummel, F., 1982. Hydrofracturing stress measurements in the Iceland research drilling project drill hole at Reydarfjordur, Iceland. Journal of Geophysical Research, 87, 6631-6649.

Hartley, M.E., Thordarson, T., 2012. Formation of Öskjuvatn caldera at Askja, North Iceland: Mechanism of caldera collapse and implications for the lateral flow hypothesis. Journal of Volcanology and Geothermal Research 227, 85-101.

Hartley, M.E., Thordarson, T., 2013. The 1874-1876 volcano- tectonic episode at Askja, North Iceland: Lateral flow revisited. Geochemistry, Geophysics, Geosystems, 14 , 2286-2309

Hildreth, W., Fierstein, J., 2012. The Novarupta-Katmai eruption of 1912—largest eruption of the twentieth century; centennial perspectives: U.S. Geological Survey Professional Paper 1791, 259 pp.

Holohan, E.P., Troll, V.R., Walter, T.R., Munn, S., McDonnell, S., Shipton, Z.K., 2005. Elliptical calderas in active tectonic settings: an experimental approach. Journal of Volcanology and Geothermal Research, 144, 119-136.

Jaeger, J.C., Cook, N.G.W., 1979. Fundamentals of Rock Mechanics, 3rd ed. Chapman and Hall, London.

Kanamori, H., Anderson, D.L., 1975. Theoretical basis of some empirical relations in seismology. Bulletin of the Seismological Society of America, 65, 1074-1095.

Kondepudi, D., 2008. Introduction to Modern Thermodynamics. Wiley, New York.

Kress, V.C., Carmichael, I.S.E., 1991. The compressibility of silicate liquids containing Fe2O3 and the effect of composition, temperature, oxygen fugacity and pressure on their redox states. Contributions to Mineralogy and Petrology, 108, 82–92.

Kusumoto, S., Takemura, K., 2005. Caldera geometry determined by the depth of the magma chamber. Earth Planets Space, 57, e17-e20.

Kusumoto, S., Gudmundsson, A., 2009. Magma-chamber volume changes associated with ring-fault initiation using a finite-sphere model: Application to the Aira caldera, Japan. Tectonophysics, 471, 58-66.

Lamb, H., 1932. Hydrodynamics, 6th ed. Cambridge University Press, Cambridge.

Lipman, P.W. 1997. Subsidence of ash-flow calderas: relation to caldera size and magma chamber geometry. Bulletin of Volcanology, 59, 198-218.

Maaloe, S., Scheie, A., 1982. The permeability controlled accumulation of primary magma. Contributions to Mineralogy and Petrology, 81, 350-357.

Macedonio G., Neri, A., Martì, J., Folch, A., 2005. Temporal evolution of flow variables during sustained magmatic explosive eruptions, Journal of Volcanology and Geothermal Research, 143, 153-172.

Machado, F., 1974. The search for magmatic reservoirs. In: Civetta, L., Gasparini, P., Luongo, G., Rapolla, A. (eds.), Physical Volcanology, Elsevier, Amsterdam, pp. 255-273.

MacLeod, C.J., Yaouancq, G., 2000. A fossil melt lens in the Oman ophiolite: implications for magma chamber processes at fast spreading ridges. Earth and Planetary Science Letters, 176, 357-373.

Malfait, W.J., Sanchez-Valle, C., Ardia,P., Médard, E., Lerch, P., 2011. Compositional dependent compressibility of dissolved water in silicate glasses.American Mineralogist, 96, 1402–1409.

Marsh, B.D., 2000. Magma chambers. In: Sigurdsson, H. (ed.), Encyclopedia of Volcanoes. Academic Press, New York, pp. 191-206.

McKenzie, D.P., 1984. The generation and compaction of partially molten rocks. Journal of Petrology, 25, 713-765.

Marti, J., Gudmundsson, A., 2000. The Las Canadas caldera (Tenerife, Canary Islands): Example of an overlapping collapse caldera generated by magma-chamber migration. Journal of Volcanology and Geothermal Research, 103, 161-173.

Marti, J., Ablay, G.J., Redshaw, L.T., Sparks, R.S.J., 1994. Experimental studies of collapse calderas. Journal Geological Society London, 151, 919-929.

Marti J., Folch, A., Neri, A., Macedonio, G., 2000. Pressure evolution during explosive caldera-forming eruptions. Earth and Planetary Science Letters, 175, 275-287.

Marti, J., Geyer, A., Folch, A., Gottsmann, J., 2008. A review on collapse caldera modelling. In: Gottsmann, J. and Marti, J. (eds), Caldera Volcanism: Analysis, Modelling and Response. Elsevier, Amsterdam, pp 233-283

Marti, J., Geyer, A., Folch, A., 2009. A genetic classification of collapse calderas based on field studies, and analogue and theoretical modelling. In: Thordarson, T., Self, S. (eds), Volcanology: the Legacy of GPL Walker. IAVCEI-Geological Society of London, London, pp. 249-266.

Milne-Thompson, L.M., 1996. Theoretical Hydrodynamics, 5th ed. Dover, New York.

Munro, D.C., Rowland, S.K. 1996. Caldera morphology in the western Galapagos and implications for volcano eruptive behaviour and mechanisms of caldera formation. Journal of Volcanology and Geothermal Research, 72, 85-100.

Murase, T., McBirney, A.R., 1973. Properties of some common igneous rocks and their melts at high temperatures. Geological Society of America Bulletin, 84, 3563-3592.

Mutter, J. C., Carbotte, S. M., Su, W. S., Xu, L. Q., Buhl, P., Detrick, R. S., Kent, G. M., Orcutt, J. A., Harding, A. J. 1995. Seismic images of active magma systems beneath the East Pacific Rise between 17-Degrees-05's and 17-Degrees-35's. Science, 268, 391-395.

Newhall, C.G., Dzurisin, D., 1988. Historical Unrest of Large Calderas of the World. U.S. Geological Survey Bulletin 1855, Reston, VA.

Newhall, C., Hendley II, J.W., Stauffer, P.H., 1997. The Cataclysmic 1991 Eruption of Mount Pinatubo, Philippines. U.S. Geological Survey Fact Sheet 113-97.

Ochs, F.A., Lange, R.A., 1997. The partial molar volume, thermal expansivity, and compressibility of H2O in NaAlSi3O8 liquid: new measurements and an internally consistent model. Contributions to Mineralogy and Petrology, 129, 155-165.

Pinel, V., Jaupart, C., 2005. Caldera formation by magma withdrawal from a reservoir beneath a volcanic edifice. Earth and Planetary Science Letters, 230, 273-287.

Pollard, D.D., Delaney, P.T., Duffield, W.A., Endo, E.T., Okamura, A.T., 1983. Surface deformation in volcanic rift zones. Tectonophysics, 94, 541-584.

Radebaugh, J., Keszthelyi, L., McEwen, A. and the Galileo SSI Team, 2000. Characteristics of calderas on Io: surface morphology, sizes, and distribution. Lunar and Planetary Sciences, 31, 1983.

Savin, G.N., 1961. Stress Concentration Around Holes. Pergamon, New York.

Seifert, R., 2013 Compressibility of Volatile-bearing Magmatic Liquids. PhD Thesis, ETH, Zurich.

Self, S., Rampino, M.R., Newton, M.S., Wolff, J.A., 1984 Volcanological study of the great Tambora eruption of 1815. Geology, 12, 659-663.

Schultz, R.A., 1995. Limits on strength and deformation properties of jointed basaltic rock masses. Rock Mech. Rock Eng. 28, 1-15.

Singh, S.C., Crawford, W.C., Carton, H., Seher, T., Combier, V., Cannat, M., Canales, J.P., Dusunur, D., Escartin, J., Miranda, J.W., 2006. Discovery of a magma chamber and faults beneath Mid-Atlantic Ridge hydrothermal field. Nature, 442, 1029-1032.

Sinton, J.M., Detrick, R.S., 1992. Mid-ocean magma chambers. Journal of Geophysical Research, 97, 197-216.

Stothers, R.B., 1984, The great Tambora eruption in 1815 and its aftermath. Science, 224, 1191-1198.

Wadge, G., 1981. The variation of magma discharge during basaltic eruptions. Journal of Volcanology and Geothermal Research, 11, 139-168.

Wood, C.A., Kienle, J., 1992. Volcanoes of North America: United States and Canada: The United States and Canada. Cambridge University Press, Cambridge.

Woods, A.W., Huppert, H.E., 2003. On magma chamber evolution during slow effusive eruptions. Journal of Geophysical Research, 108, No. B8, 2403, doi: 10.1029/2002JB002019.